Computers and Concrete, *Vol. 20, No. 3 (2017) 339-350*
DOI: https://doi.org/10.12989/cac.2017.20.3.339

Dynamic bending behaviours of RC beams under monotonic loading with variable rates

Shiyun Xiao*[1], Jianbo Li[1a] and Yi-Lung Mo[2b]

[1]*State Key Laboratory of Coastal and Offshore Engineering, Dalian University of Technology, China*
[2]*Department of Civil and Environmental Engineering, University of Houston, USA*

(Received September 27, 2016, Revised April 12, 2017, Accepted May 10, 2017)

Abstract. Dynamic behaviours of reinforced concrete (RC) bending beams subjected to monotonic loading with different loading rates were studied. A dynamic experiment was carried out with the electro-hydraulic servo system manufactured by MTS (Mechanical Testing and Simulation) Systems Corporation to study the effect of loading rates on the mechanical behaviours of RC beams. The monotonic displacement control loading, with loading rates of 0.1 mm/s, 0.5 mm/s, 1 mm/s, 5 mm/s and 10 mm/s, was imposed. According to the test results, the effects of loading rates on the failure model and load-displacement curve of RC beams were investigated. The influences of loading rates on the cracking, ultimate, yield and failure strengths and displacements, ductility and dissipated energy capability of RC beams were studied. Then, the three-dimensional finite element models of RC beams, with the rate-dependent DP (Drucker-Prager) model of concrete and three rate-dependent model of steel reinforcement, were described and verified using the experimental results. Finally, the dynamic mechanical behaviours and deformation behaviours of the numerical results were compared with those of the experimental results.

Keywords: reinforced concrete (RC) beam; loading rate; strength; deformation; ductility; numerical simulation

1. Introduction

The dynamic behaviour of reinforced concrete (RC) members, such as RC beams and RC columns, is inevitably affected by loading rate. On the one hand, concrete and steel are typical rate-dependent materials: their strengths, stiffness and brittleness (or ductility) are affected by loading rate. On the other hand, the failure mode of RC members due to dynamic load is different from that of static load. With the exception of the familiar flexural failure, the brittle shear failure may occur under some circumstances, even though RC members are designed according to the flexural failure; in other words, shear failure occurs before flexural failure. This phenomenon has been confirmed through the dynamic tests of RC members (Ghabossi 1984, Krauthammer 1984, Krauthammer 1986).

Research regarding the rate-dependency of concrete started in 1917 with Abrams' dynamic compressive experiment (Abrams 1917); since then, increasing numbers of researchers have focused their interests on the dynamic behaviour of concrete and some accepted conclusions have been drawn, such as the tensile and compressive strength of concrete increased with the increasing strain rate. Although some researchers do not agree regarding which strain rates cause an increase in strength to become significant, the conclusion that there is a definite increase in the uniaxial compressive strength of concrete with increasing strain rates has been generally accepted. However, confusion has arisen regarding the increase in the magnitude of dynamic strength. Some experimental results (Abrams 1917, Jones 1936, Watstein 1953, Rush 1960, Atchley 1967, Spooner 1972, Hughes 1972, Sparks 1973, Dilger 1984) have shown an increase of 30 percent more than the static strength of concrete and even up to 80 percent, while for others (Evans 1942, Dhir 1972), the increase in the strength of concrete was less than 20 percent and was not influenced by the rate of loading. Bischoff *et al.* (1991) reviewed and analysed the dynamic compressive experiments of concrete and deduced that the confusion regarding the increase magnitude of dynamic strengths arose because many factors, such as concrete quality, aggregate, age, curing, and moisture conditions, influence the behaviour during rapid loading. The dynamic tensile tests of concrete reported in the literature were more difficult to perform and the results were few. Birkimer *et al.* (1971) conducted two sets of dynamic tensile tests using plain concrete cylinders. Zielinski *et al.* (1981) studied the behaviour of concrete that was subjected to uniaxial impact tensile loading and found that the ratios of impact and static tensile strengths were between 1.33 and 2.34 for different concrete mixes. Oh (1987) presented a realistic nonlinear-stress-strain model that can describe the dynamic tensile behaviour of concrete. Tedesco *et al.* (1991) conducted direct tension tests of plain concrete specimens on a split-Hopkinson pressure bar to investigate the effects of increasing strain rate on the tensile strength of concrete. Rossi *et al.* (1994) made an experimental study of rate effects on the behaviour of concrete under tensile stress to investigate the effect of the water/cement ratio on tensile strength enhancement.

*Corresponding author, Professor
E-mail: shyxiao@dlut.edu.cn
[a]Associate Professor
[b]Professor

ISSN: 1598-8198 (Print), 1598-818X (Online)

Moreover, analysis of the physical mechanisms was developed to investigate how the Stefan effect, the cracking process, and the inertia forces participated together in the dynamic behaviour of a specimen subjected to a uniaxial tensile test (Rossi *et al.* 1996). Malvar (1998) reviewed the extant data characterizing the effects of strain rate on the tensile strength of concrete and compared the DIF formulation with that recommended by the European CEB (1998). Finally, an alternative formulation was proposed based on the experimental data. Cadoni *et al.* (2001) studied the effect of strain rate on the tensile behaviour of concrete at different relative humidity levels.

Recently, more and more researchers have studied the effect of loading rate on the dynamic behaviour of RC members. Krauthammer *et al.* (1984) presented a method for the analysis of reinforced concrete box-type structures under the effect of severe dynamic loading conditions, demonstrated by employing it for the analysis of seven different events and then evaluating its accuracy by comparing numerical and experimental results (Krauthammer *et al.* 1986). Afterward, with the rate-dependent model compared with the rate-independent model, the dynamic responses of RC beams under the dynamic loading condition were further studied (Beshara 1992, Al-Haddad 1995, Farag 1996, Kulkarni 1998). Kunnath (Kunnath *et al.* 1990) presented an efficient model for inelastic biaxial bending interaction of RC sections and then demonstrated the validity of the proposed scheme through the analytical simulation of available biaxial experiments on RC columns in comparison with other analytical models. Fu *et al.* (1991) presented a survey on the behaviour of RC subjected to dynamic loading, reviewing and then discussing the response of RC materials and elements to various strain rates. As the rate of loading increased, the concrete compressive strength, steel yield strength and flexural capacity of the RC members also increased. If significant, the increase in the flexural capacity of individual members as a result of high strain rates might transform a structure's failure mode from a preferred ductile manner to a less desirable brittle mode. A rate- and history-dependent constitutive model of concrete was developed to nonlinearly analyse both the plane and axisymmetric RC structures subjected to transient impulsive loading (Beshara *et al.* 1992). Considering the actual properties of the reinforcing steel under both low and high strain rates of loading, Al-Haddad (1995) undertook a parametric study of the curvature ductility capacity of RC sections. The results indicated that using the ACI code-specified yield strength of the reinforcing steel led to overestimating the ductility capacity of the RC sections. Farag *et al.* (1996) proposed an improved material model for concrete, which included the effect of high strain rate upon both the stiffness of the material and upon the crushing strength, and the expressions for the yield and failure surfaces of concrete, which account for the effects of high strain rate. Next, this material model was incorporated into an existing finite element program to compare with a series of test results. Seven pairs of singly reinforced beams (without shear reinforcement) were tested under displacement control with a closed-loop servo-hydraulic testing machine to investigate the dynamic behaviour of RC beams at high rate of loading (Kulkarni *et al.* 1998). To improve the computational efficiency in the transient dynamic non-linear analysis of RC plates subjected to blast or seismic loading, a parallel scheme for the time marching procedure using the explicit Newmark's algorithm was presented (Sziveri *et al.* 1999).

Nürnbergerová *et al.* (2001) presented a theoretical model for the determination of the moment vs. curvature and shear force vs. shear deformation relationships based on the stress-strain curves of the materials. A comparison of the theoretical values against the test results for reinforced beams subjected to the concentrated load showed good agreement for both the curvature and shear deformations. Fujikake developed an analytical model based on a fibre model technique for representing the behaviour of a reinforced Reactive Powder Concrete (RPC) beam subjected to rapid flexural loads (Fujikake *et al.* 2006a) and experimentally examined the impact response of a RPC beam and developed an analytical model to represent its impact response (Fujikake *et al.* 2006b). To study the relationship between the nonlinear dynamic behaviour of RC beams and their damage levels, the time-frequency response analyses from the impact excitation vibration tests were carried out on RC beams with different damage levels (Wang *et al.* 2006). Cotsovos *et al.* (2008) described the numerical investigation into the dynamic response of RC beams subjected to high rates of transverse loading. Different from other studies, Cotsovos attributed the effect of the applied loading rate on the exhibited structural response to the inertia forces that developed within the beam instead of the loading rate sensitivity of the materials. Valipour *et al.* (2009) took into account the effect of strain rate at the fibre level by using the dynamic increase factor (DIF) concept for steel and concrete to improve upon a one-dimensional flexibility of the fibre element that ignored the shear effect at the material level. This was done to investigate the dynamic responses of RC beams and columns subjected to impact. Fujikake *et al.* (2009) examined the impact responses of RC beams through an experimental study, presenting an analytical model he developed to predict the maximum mid-span deflection and maximum impact load. Abbas *et al.* (2010) investigated key aspects of structural response, such as the load-deformation behaviour, crack patterns, and the strength and failure modes of RC wide beams under low-rate (static) and high-rate (impact) concentrated loading applied at their mid-span. An iterative approach for the computation of a curvature ductility factor for doubly RC sections was proposed by taking into account the strain rate sensitive properties of concrete and steel, the confinement of core concrete and the degradation of cover concrete during load reversal under earthquake loading (Pandey 2011). Through an experimental study, Fukuda *et al.* (2011) investigated the dynamic shear failure behaviour of RC beams under rapid loading. The results showed that the influence of the loading rate on the maximum resistance was more significant for the RC beams that failed in shear than those that failed in flexure. The behaviour of RC beams under varying rates of concentrated loading, dynamic loading and high rate loading were studied

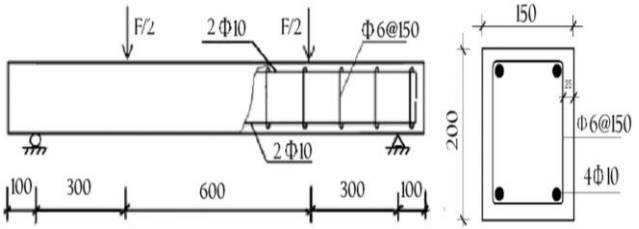

Fig. 1 Loading and reinforcement layout of RC beam

to investigate the effect of loading rate on RC beams (Adhikary *et al.* 2012, 2013, 2014). Pandey (2013) took into account the strain rate sensitive constitutive behaviour of concrete and steel to compute the flexural ductility of RC beam sections. The parametric studies indicated that the flexural ductility factor decreased with increasing strain rates. Li *et al.* (2013) studied the effect of loading rate on RC beams experimentally and numerically at strain rates in the range of 10^{-5} and 0.1/s that could potentially be experienced during earthquakes. Afterwards, the dynamic behaviour of RC beams was given through experiments and the effects of loading rate on the bearing capacity, ductility, stiffness, failure mode and energy dissipation capacity of beams were analysed.

These studies indicated that the effects of loading rates on the dynamic behaviours of RC members were not negligible. However, only few design codes have taken account into the effects of loading rates on the RC structures because the study on the effects of loading rates was not enough and the results are still not accepted by most engineers. In this paper, a dynamic experiment of reinforced concrete beams at different loading rates was carried out to study the effects of loading rates on the mechanical behaviours of RC beams. According to the test results, the effect of loading rates on the failure shape and loading-displacement curve of RC beams was investigated. The cracking, yield, ultimate and failure strengths and deformation, ductility and dissipated energy capability of RC beams were studied. Finally, to verify the experimental results, the two-dimensional finite element models of RC beams were compared with the rate-dependent DP model of concrete and two rate-dependent model of steel reinforcement.

2. Experimental investigation

2.1 Beam design and material properties

The test RC beams were designed based on the consideration of the fundamental period of the beams, consistent with that of general concrete buildings. Each of the RC beams, with dimensions 1400 mm in length, 150 mm in width and 200 mm in depth, was simply supported within a 1200 mm span, as shown in Fig. 1. Portland cement was used in all the mixtures; its concrete grade was designed to be 25 MPa. The mix proportion of constituents by weight was 1.00: 0.40: 1.18: 2.36, which corresponded to cement, water, sand and gravel, respectively. According to the Code for Design of Concrete Structures (GB 50010-2010), the average 28-day concrete cube compressive strength for all the beams was 25 MPa. The tensile strength was adopted as one tenth of the compressive strength. The longitudinal steel reinforcement consisted of four rebars, 10 mm in diameter, horizontally placed in the top and bottom of the beam. The transverse stirrups were 6 mm in diameter and 150 mm in distributed distance. The design yield strength of reinforcing bars of the RC beams was 320 MPa.

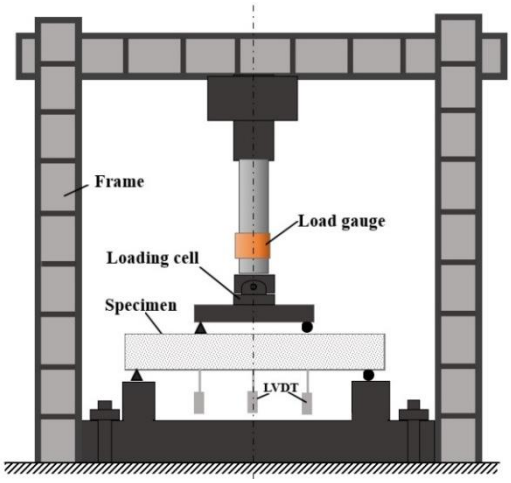

(a) Loading system

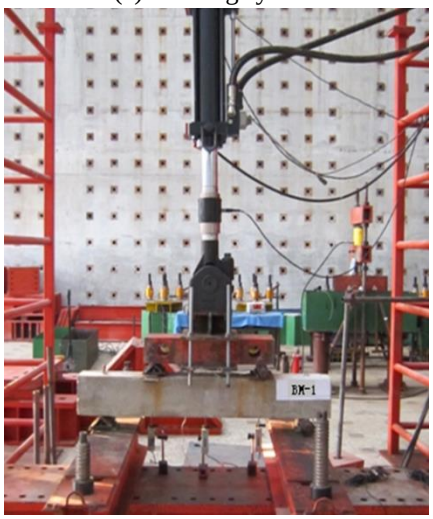

(b) Setup

Fig. 2 Loading equipment and test setup

2.2 Loading setup and loading program

The tests were carried out in the structural laboratory at Shenyang Jianzhu University, China. The multi-channel MTS servo-hydraulic loading system was employed for loading. The maximal thrust loading was up to 350 kN, the maximal push loading was up to 240 kN and the maximal displacement was up to 500 mm. The stiffness of the test frame for RC beams needed to be sufficient to reduce the measurement error. To avoid a local failure of the boundary concrete, two 20-mm depth armour plates were imbedded into the bottom and the top of the RC beams to support the beam and the loading steel beam. The setup and the loading equipment are shown in Fig. 2.

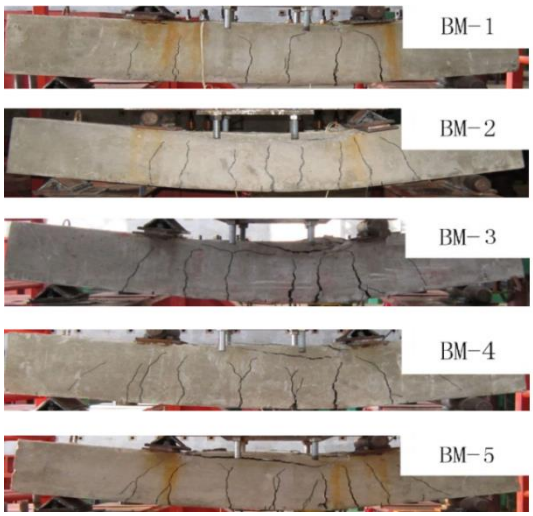

Fig. 3 Failure mode of beams at various loading rates

To study the effect of loading rate on the dynamic behaviour of RC beams, a displacement-controlled monotonic load with different loading rates, i.e., 0.1, 0.5, 1, 5 and 10 mm/s, was imposed on five beams: BM-1, BM-2, BM-3, BM-4 and BM-5, respectively.

2.3 Measurement setup

Because the maximum loading rate was 10 mm/s, a high-speed data acquisition system was needed to prevent the test data from being lost. The dynamic data acquisition system DH5937 was therefore utilized in this experiment. The system collected different electrical signals, with a maximum acquisition frequency of 20 kHz. All 8 channels worked at the same time and the simultaneous collection frequency of every channel could achieve 2.5 kHz. To collect sufficient, but not overabundant, data, various collection frequencies were adapted at various loading rates. The collection frequencies of five test beams BM-1, BM-2, BM-3, BM-4 and BM-5 were 20, 50, 200, 1000 and 2000 Hz, respectively. During the tests, the strain of reinforcements, the mid-span displacement of the beam and the MTS loading actuator were acquired.

3. Experimental results

3.1 Failure analysis of RC beams

The experiment was designed to study the effect of loading rate on the dynamic behaviours of the pure bending segment. The crack pattern and failure configuration of RC beams at various loading rates are shown in Fig. 3. The failure configurations were the same at various loading rates, and tensile-failed concrete caused the vertical cracks of concrete located at the bottom of the beam. Through careful observation and comparison, the width of the crack decreased slightly with increasing loading rates; they also distributed more uniformly when the displacement was the same. The reason for this might be that the rapid loading rate delayed the propagation of any internal micro-cracks

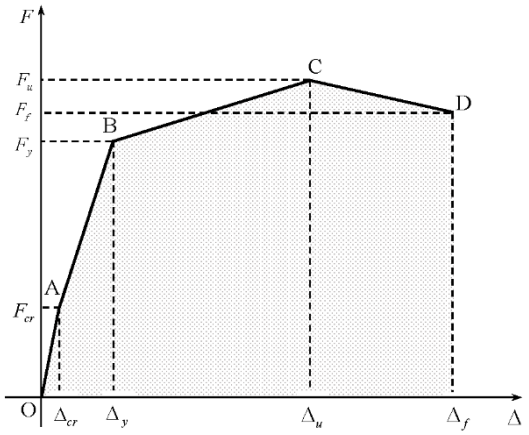

Fig. 4 The sketch map of the loading-displacement curve

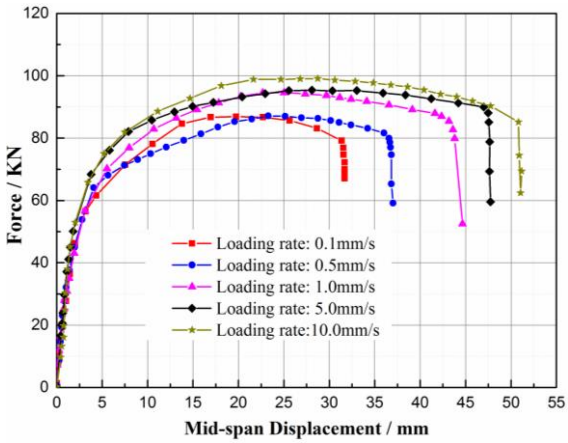

Fig. 5 The mid-span loading-displacement curves at various loading rates

and enlarged the crack field, which caused the developments of the external cracks. Consequently, when the displacements for all the RC beams were the same, more visible cracks appeared and the crack width decreased with increasing loading rate.

3.2 Effect of loading rates on the loading-displacement curves

The mid-span loading-displacement curve was an important factor in evaluating the mechanical behaviours of the simply supported RC beam. Fig. 4 plots the sketch map of the loading-displacement envelope curve for RC beams. Generally, the plot consists of four segments. The first straight line shows the linear behaviour before the first crack (point A). The second slope, corresponding to the cracked section, followed until point B, where the flexural reinforcement yielded. At point B, the displacement of the beam began to increase at a higher rate as greater loads were applied. After point B, the nonlinearity of the RC beams appeared obviously because the cracked concrete and the yielding reinforcement led to the degradation of the RC beam's stiffness. The beam's stiffness descended to zero at point C, where the ultimate loading corresponded to the nominal flexural capacity of the cross-section. After point C, the beam's ability to distribute the load throughout the

Table 1 Crack, yield, ultimate and failure strength

Strength (kN)	BM-1	BM-2	BM-3	BM-4	BM-5
Cracking	24.48	25.65	26.12	27.85	27.93
Yield	61.38	64.29	68.77	70.82	71.11
Ultimate	87.51	88.34	94.98	95.59	99.20
Failure	79.20	81.67	85.46	90.00	85.14

cross-section began to decrease with increasing deformation until the failure point D.

Fig. 5 illustrates the five mid-span load-displacement envelope curves of the RC beams subjected to various loading rates. Compared with the five curves, it could be found that at the beginning of the load, the reinforced steel and concrete were within their elastic stages. The loading-displacement curves appeared as a straight line and the effect of the loading rate was negligible. With increasing loading rate, the effects of loading rates on the concrete and steel became more obvious and the loading-displacement curve appeared as the nonlinear arity. Thus, the yielding loading, the ultimate loading, and the corresponding yield and ultimate displacement increased distinctly.

3.3 Influence of loading rates on the crack, yield, ultimate and failure strength

The crack strength, the yield strength, the ultimate strength and the failure strength were defined as the carrying ability of point A, B, C and D of RC beams in Fig. 4, respectively.

Table 1 lists the crack strength, the yield strength, the ultimate strength and the failure strength of RC beams at various loading rates. From the table, it is clear that the crack strength, the yield strength, the ultimate strength and the failure strength likewise increased with increasing loading rates. When compared with specimen BM-1, the crack strengths of specimens BM-2, BM-3, BM-4 and BM-5 increased by 4.78, 6.70, 13.77 and 14.09%, respectively. Similarly, the yield strengths of specimens BM-2, BM-3, BM-4 and BM-5 increased by 4.74, 12.04, 15.38 and 15.85%, the ultimate strength increased by 0.95, 8.54, 9.23 and 13.36%, and the failure strength increased by 3.12, 7.90, 13.64 and 7.50%, respectively.

According to reference (Bischoff *et al.* 1991), the increase in concrete strength followed a linear-logarithmic relationship with the increase in loading rate. Similarly, Fig. 6 illustrates the relationship between the crack, yield and ultimate strength of RC beams and the logarithm to 10 of the loading rate. It was concluded that the crack strength, the yield strength and the ultimate strength increased notably. Compared with the crack strength, the slopes of the yield and ultimate strength were somewhat larger than that of the crack strength. The reason for this was that the effects of the loading rate on concrete and steel reinforcement were different at various stages. Most of the loading was carried by the concrete before it cracked; thus, the effect of the loading rate on the crack loading of the RC beam was close to the effect on the concrete. In the yield and ultimate states, most of the tensile loading at the bottom of the beam was carried by the tensile steel reinforcement; however, most of

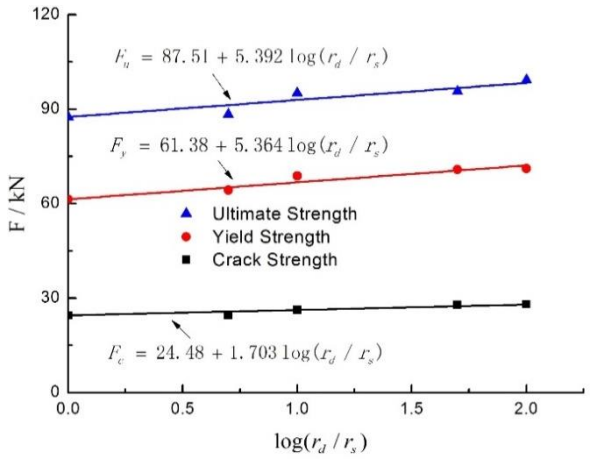

Fig. 6 Relationship between the loading and the logarithmic of the loading rate

Table 2 Crack, yield, ultimate and failure displacement

Displacement (mm)	BM-1	BM-2	BM-3	BM-4	BM-5
Cracking	0.59	0.62	0.69	0.74	0.78
Yield	3.40	3.52	3.78	3.98	4.05
Ultimate	19.74	23.29	25.02	25.56	26.80
Failure	31.37	36.01	43.17	47.01	50.82

the compressive loading at the top of the beam was carried by the compressive concrete; thus, the effect of the loading rate on the yield and ultimate strength of the RC beams was determined by the combined effects of the loading rate on the concrete and steel reinforcement. Obviously, the combined effects were stronger than those on the crack strength of the RC beam.

3.4 Effect of loading rates on the deformation behaviour

The mid-span crack, yield, ultimate and failure displacement at different loading rates are listed in Table 2. It was also concluded that the mid-span crack displacement, the yield displacement, the ultimate displacement and the failure displacement of the RC beam increased obviously with increasing loading rate. Compared with beam BM-1, the mid-span crack displacement of beams BM-2, BM-3, BM-4 and BM-5 increased by 5.1, 16.9, 25.4 and 32.2%, respectively. Similarly, the mid-span yield displacement of beams BM-2, BM-3, BM-4 and BM-5 increased by 3.5, 11.2, 17.1 and 19.1%, the mid-span ultimate displacement increased by 17.2, 39.4, 51.6 and 57.9%, and the failure displacement increased by 14.79, 37.62, 49.86 and 62.00%, respectively. These test results were in agreement with the previous test of reinforced concrete members (Li *et al.* 2013).

3.5 Effect of loading rates on the displacement ductility factor

Ductility characterizes the deformation capacity of members (structures) after yielding, i.e., their ability to

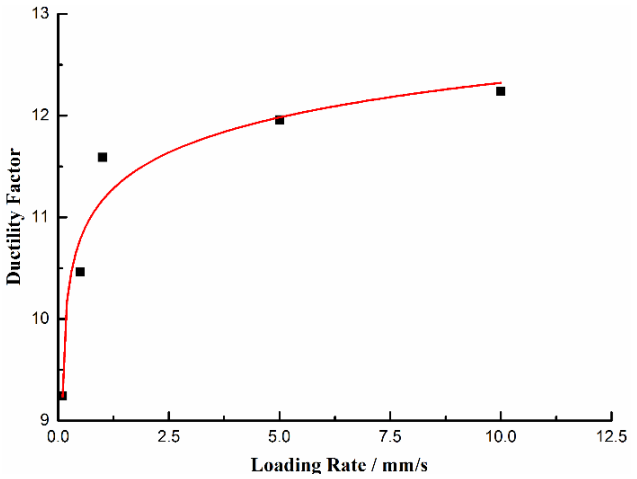

Fig. 7 The displacement ductility factor curves with the loading rate

dissipate energy. In this paper, the displacement ductility factor is defined as the ratio of the deformation in the failure state to that in the yield state, as follows

$$\mu_{\Delta} = \frac{\Delta_f}{\Delta_y} \tag{1}$$

where Δ_y is the mid-span displacement of the RC beam in the yield state and Δ_f is that in the failure state.

Fig. 7 lists the displacement ductility factor curves with the loading rate. It was clear that the displacement ductility factor increased obviously with increasing loading rate, which was contrary to Al-Haddad's results (Al-Haddad 1995). The reason might be that Al-Haddad's results did not consider the effect of strain rate on the deformation behaviours of concrete and the steel reinforcement.

3.6 Effect of loading rates on the energy dissipation capacity

One of the most important aspects of structural performance under seismic loading is the ability of a structure to adequately dissipate energy. The energy dissipation capacity of the RC beam was defined by the capacity to absorb the energy dissipated by concrete and reinforcing steel in one loading process. The energy dissipation capacity was obtained by calculating the area under the load vs. mid-span displacement curve, as listed in Fig. 4. Generally, energy dissipation capacity depended on different parameters, such as reinforcement ratio, arrangement of reinforcing bars, and shape and size of the members' cross-sections. The energy dissipation of the RC beams at various loading rates is listed in Fig. 8. It is clear that the energy dissipation capacity increased dramatically with increasing loading rate. Compared with beam BM-1, the energy dissipation capacity of beams BM-2, BM-3, BM-4 and BM-5 increased by 17.01, 53.94, 72.20 and 90.04%, respectively. The energy dissipation capacity was enhanced because increasing the loading rate not only increased the crack, yield and ultimate strength of the RC beams but also improved the RC beams' deformation ability.

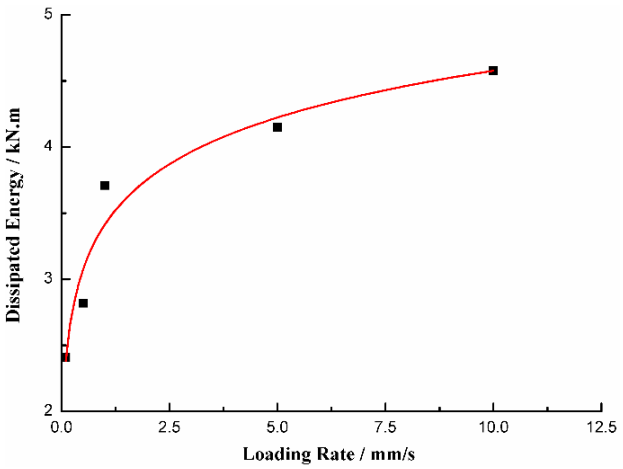

Fig. 8 The dissipated energy with the loading rate

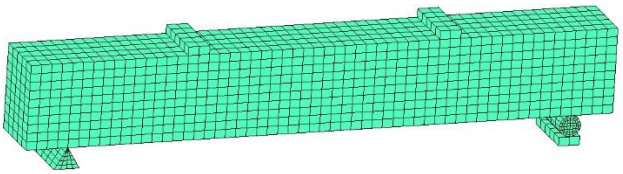

Fig. 9 The FE model of tested RC bending-beams

4. Numerical analysis of rc beams

To analyse the effect of loading rates on the dynamic behaviours of RC beams, numerical simulation of the dynamic experiment was carried out with the MSC.Marc software and the user subroutine UVSCPL. The numerical results were verified and compared with the experimental results.

4.1 Structural geometry

The three-dimensional FE model of the tested RC bending-beams was adopted to simulate the test, as shown in Fig. 9. Eight node solid elements with 3×3×3 Gauss quadrature integration points were used to represent concrete, while two-node rebar elements were used to model the steel reinforcing rebar. A mesh size of 10 mm×10 mm×10 mm was used to create the solid element of the RC beam. The rebar membrane elements were inserted into the host concrete elements; their lengths were 10 mm.

4.2 Boundary conditions and application of load

To simulate the actual experimental conditions, the beams were supported on one rigid prismy plate and one rigid cylinder roller made of solid elements. Displacement loading was prescribed in the rigid loading plates located on the top of the RC beam. The rigid prismy plate and the cylinder roller were discretized into 4-node solid elements. The monotonic linear displacement loading was adapted. Displacement loading controlled by the loading rate according to the experimental program was imposed on the rigid plates.

4.3 Modelling of materials

Table 3 Compressive strength and DIFs of concrete

Loading rate (mm/s)		0.1	0.5	1	5	10
Ultimate strength (MPa)	1	25.58	27.10	26.50	30.75	32.33
	2	24.48	26.31	29.15	30.79	32.18
	3	24.19	25.60	27.02	31.44	32.05
	Avg	24.75	26.34	27.56	30.99	32.19
	DIF	1.00	1.06	1.11	1.25	1.30

4.3.1 Concrete

The consistency viscoelastic Drucker-Prager (DP) model of concrete (Xiao *et al.* 2008) was adopted in this paper. It could be seen as an extension of the classic elasto-plastic DP model to account for the rate-dependent behaviour of materials.

In this model, the yield surface function was assumed to be the same as the failure surface function of concrete; thus, the yield function of the Drucker-Prager model could be expressed as

$$\varphi = \sqrt{3J_2} + \alpha I_1 - k = 0 \tag{2}$$

where two parameters α, κ were chosen based on two conditions: 1) uniaxial tensile strength f_t; 2) uniaxial compressive strength f_c.

It was deduced that

$$\alpha = \frac{f_c - f_t}{f_c + f_t} \qquad k = \frac{2 f_c f_t}{f_c + f_t} \tag{3}$$

The compressive strengths and DIFs at the various strain rates were given in Table 3. According to the Code for Design of Concrete Structures (GB 50010-2010), the tensile strength of concrete was chosen as one tenth of compressive strength in this paper. Other material parameters of concrete came from the reference (Xiao *et al.* 2008).

To study the crack and failure behaviour of the RC beam at different stages, the crack model of concrete was chosen. The tensile strength was defined as the critical stress, the softening modulus was adopted as one-fifth of the initial elastic modulus and the shear retention was 0.5.

4.3.2 Steel reinforcement

The trilinear elastic-plastic model of reinforced rebar was adopted and some basic material parameters of steel reinforcement were chosen based on Li's dynamic experimental results (Li *et al.* 2010). The effect of loading rates on the yield strength and ultimate strength was presented by the dynamic increase factor (DIF).

Similar to the dynamic test of RC beams, the dynamic test of steel reinforcement was carried out to measure the DIFs of the yield and ultimate strengths at various loading rates, as listed in Table 4.

Malvar (1998) studied the strength enhancement of steel reinforcing bars under the effect of high strain rates. This was described in terms of the DIF, which could be evaluated for different steel grades and for yield stresses, f_{ys}, ranging from 290 to 710 MPa, as

Table 4 Strength and DIFs of the steel reinforcement

Loading rate (mm/s)		0.1	0.5	1	5	10
Yield strength (MPa)	1	292.8	314.4	314.9	322.2	380.6
	2	305.8	310.5	312.9	331.3	373.2
	3	295.9	315.2	316.1	326.8	370.8
	Avg	298.2	312.1	313.8	326.8	376.9
	DIF	1.0	1.047	1.052	1.096	1.264
Ultimate strength (MPa)	1	389.0	399.5	423.8	427.3	453.6
	2	405.5	400.9	409.6	428.6	447.9
	3	401.8	417.7	421.4	422.7	449.1
	Avg	398.8	406.0	418.3	426.2	450.2
	DIF	1.0	1.018	1.049	1.069	1.129

Table 5 Mid-span displacement rate of RC beams and strain rate of steel reinforcement

Loading rate (mm/s)	0.1	0.5	1	5	10
Displacement rate (10^{-3}m/s)	0.14	0.7	1.4	7	14
Strain rate (10^{-3}/s)	0.864	3.24	57.1	214	377

Table 6 Calculated models of RC beams

Model	Concrete	DIF of steel
I	Rate-independent DP	Rate-independent
II	Rate-dependent DP	Malvar
III	Rate-dependent DP	CEB
IV	Rate-dependent DP	Test

$$DIF = \left(\frac{\dot{\varepsilon}_s}{10^{-4}}\right)^{\alpha} \tag{4}$$

where, for calculating yield stress $\alpha = \alpha_{fy}$,

$$\alpha_{fy} = 0.074 - 0.04(f_{ys} / 414) \tag{5}$$

and, for ultimate stress calculation $\alpha = \alpha_{fu}$,

$$\alpha_{fu} = 0.019 - 0.009(f_{ys} / 414) \tag{6}$$

The CEB Bulletin (1988) presented several formulations for different steel types, providing DIF for yield stress and ultimate stress. In the case of hot-rolled reinforcing steel, the following expressions were provided

$$\frac{f_{yd}}{f_{ys}} = 1.0 + (\frac{6.0}{f_{ys}}) \ln(\frac{\dot{\varepsilon}_s}{\dot{\varepsilon}_{s0}}) \tag{7}$$

$$\frac{f_{ud}}{f_{us}} = 1.0 + (\frac{7.0}{f_{us}}) \ln(\frac{\dot{\varepsilon}_s}{\dot{\varepsilon}_{s0}}) \tag{8}$$

$$\dot{\varepsilon}_{s0} = 5 \times 10^{-5} / s \tag{9}$$

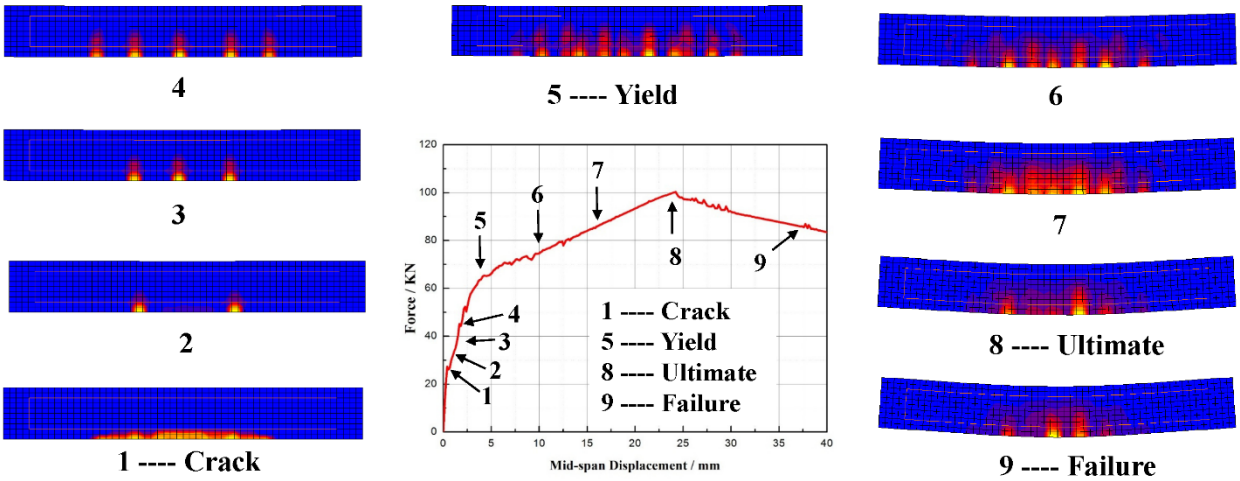

Fig. 10 Crack patterns of RC beam at different loading stages

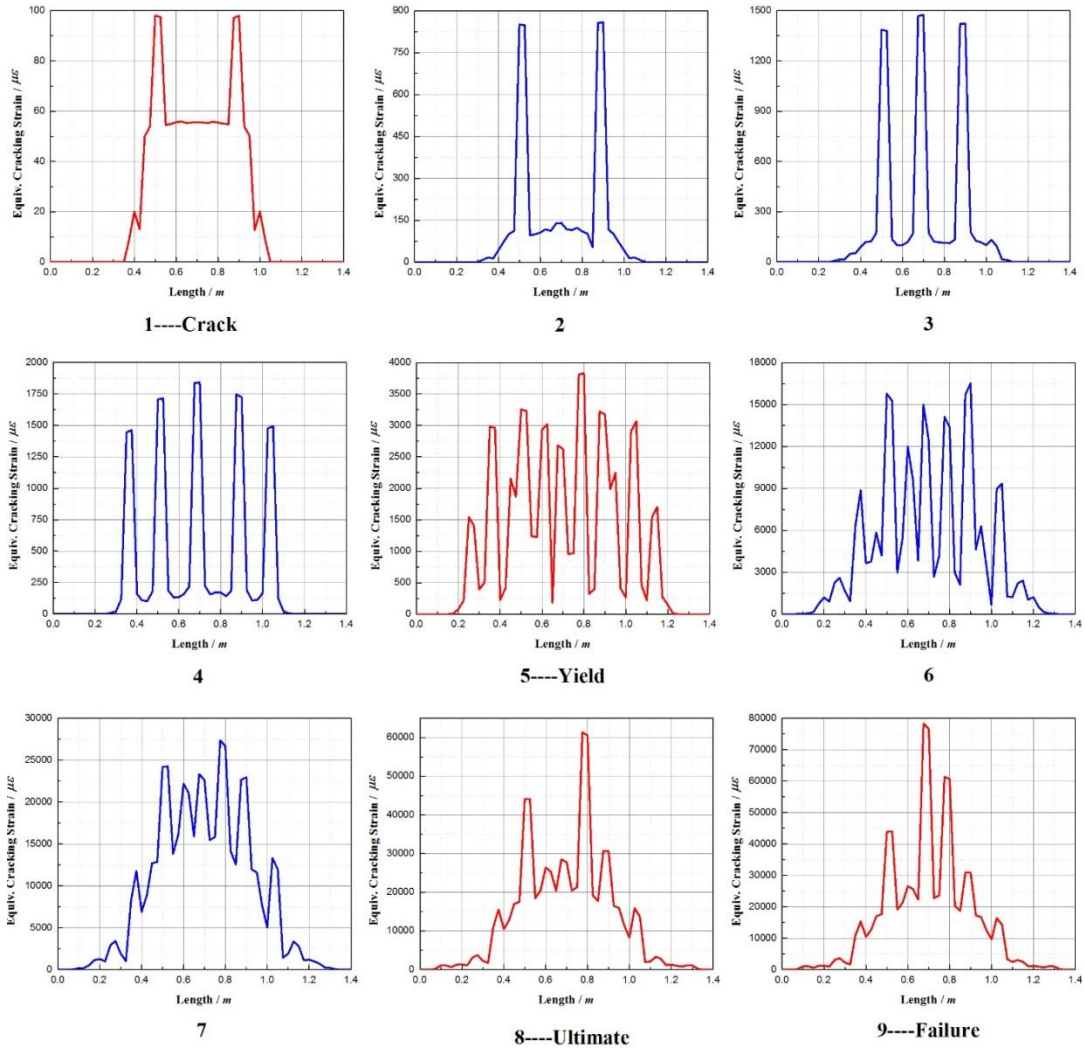

Fig. 11 Equivalent crack strain of RC beam at different loading stages

where f_{yd} is the dynamic yield stress; f_{ys} is the static yield stress; f_{ud} is the dynamic ultimate tensile stress; f_{us} is the static ultimate tensile stress; $\dot{\varepsilon}_s$ is the strain rate; $\dot{\varepsilon}_{s0}$ is a constant equal to 5×10^{-5} s^{-1} and represents strain rates in the quasi-static condition.

A comparison (Demenico *et al.* 2009) between the numerically evaluated DIFs and those obtained from the experimental results revealed that the CEB expression slightly underestimated yield stress DIF, whereas the Malvar formulation weakly overestimated it. By contrast, both expressions fitted experimental DIFs well for the

ultimate stress.

In this paper, these DIF expressions proposed by the test results, Malvar and the CEB Bulletin were adopted to study the effect of loading rates on the dynamic behaviours of RC beams.

The DIF of steel rebar was determined based on the peak strain rate. To estimate the peak strain rate of the tensile reinforcement in the mid-span, Adhikary *et al.* (2012) proposed a simplified equation by analysing the experimental result, i.e.,

$$\dot{\varepsilon}_p = 1.25 \times \dot{\delta}^{0.82} \tag{10}$$

where $\dot{\delta}$ is the mid-span displacement rate of the RC beam.

This equation could be very useful in finite element simulation of RC beams to calculate the DIF of yield and ultimate stress of tensile reinforcements under varying loading rates. The peak strain rates of the tensile reinforcement at the bottom of RC beams, shown in Table 5, were calculated according to the loading rate of the mid-span using Eq. (10).

4.4 Loading and support plate

The rigid material was used for the loading plates and the support roller and plate. Realistic values of Young's modulus of the rigid material were defined as decuple, as that of the steel material. Poisson's ratio of the rigid material should be defined as the same as that of steel material.

5. Comparison of numerical and experimental results

Four model numerical simulation results of reinforced concrete beams subjected to five various loading rates were compared with the experimental results of the present study. The effects of loading rates on the mid-span loading deformation curve, the dynamic strength, the deformation behaviour and the crack pattern were studied. Four calculated models of RC beams are listed in Table 6.

5.1 Crack process and crack strain

The crack of the RC beams by numerical simulation was shown by plotting the equivalent cracking strain. These equivalent cracking strain contours revealed the cracking strain localization where the crack would propagate. Fig. 10 showed the equivalent cracking strain contours of numerical simulation results at different stages, such as the cracking, yield, ultimate and failure states. Similar to the sketch map of the loading-displacement envelope curve in Fig. 4, the typical loading displacement curve and the whole crack process of the RC beam were illustrated (Fig. 10) and the equivalent crack strain on the bottom of the RC beam was plotted (Fig. 11). The first straight line showed the linear behaviour of the RC beam before the crack point (point 1), in which some micro-cracks firstly appeared on the bottom. With increasing load, some micro-cracks enlarged and

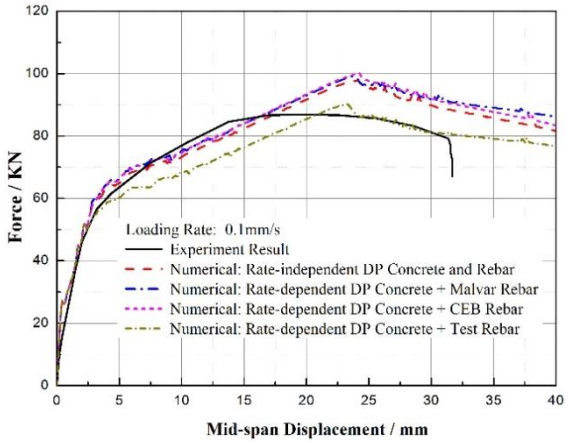

Fig. 12 Load vs. mid-span displacement curves (loading rates: 0.1 mm/s)

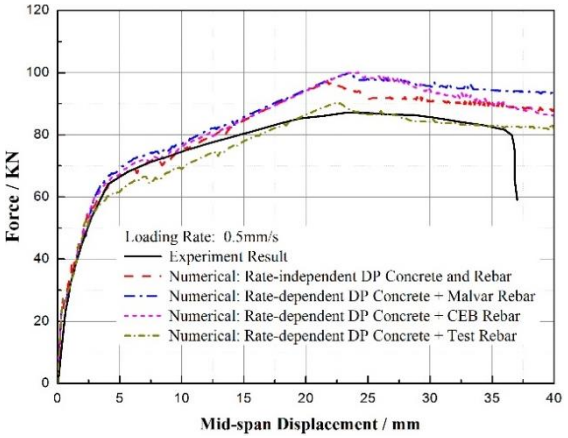

Fig. 13 Load vs. mid-span displacement curves (loading rates: 0.5 mm/s)

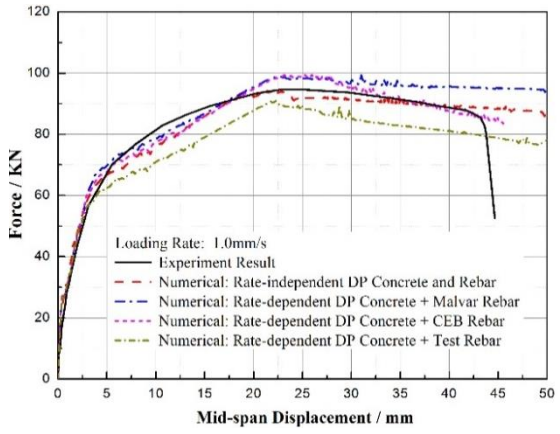

Fig. 14 Load vs. mid-span displacement curves (loading rates: 1.0 mm/s)

expanded to become macro-cracks. Two (point 2), three (point 3) and five (point 4) obvious macro-cracks appeared on the bottom of RC beam, respectively. The equivalent crack strains were up to 1000, 1500 and 1800 micro-strain, respectively. The load continued to increase, the flexural reinforcement yielded and approximately ten macro-cracks appeared on the bottom of the RC beam (point 5), at which the RC beam reached its yield strength. After point 5, the

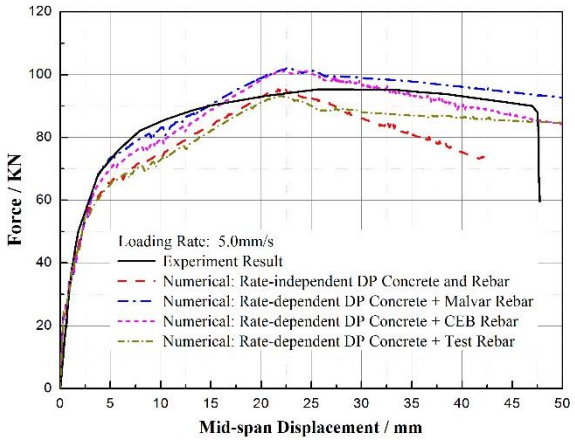

Fig. 15 Load vs. mid-span displacement curves (loading rates: 5.0 mm/s)

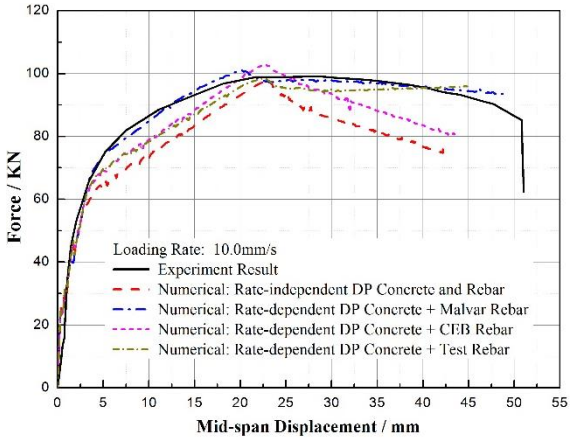

Fig. 16 Load vs. mid-span displacement curves (loading rates: 10.0 mm/s)

nonlinearity of the RC beams appeared obviously because the cracked concrete and the yielding reinforcement led to the degradation of the RC beam's stiffness. Several macro-cracks accumulated together and formed some new cracks; the equivalent crack strains were up to 15000 (point 6) and 25000 (point 7) micro-strain. With the increased load, the beam's stiffness descended to zero at the ultimate point (point 8), where the ultimate loading corresponded to the nominal flexural capacity of the cross-section. The maximal equivalent crack strain was up to 50000 micro-strain. After point 8, the beam's displacement increased but the load decreased until the failure point (point 9), at which the maximal equivalent crack strain was up to 70000 micro-strain.

5.2 Curves of loading-displacement

Figs. 12 to 16 presented the comparisons of four model numerical simulation results with experiments of load vs. mid-span displacement curves of an RC beam under five various loading rates.

From these figures, the numerical results could well describe the loading deformation behaviour of the RC beam before the yield point. After the yield point, these curves became flat because of the concrete cracking and the steel reinforcement yield. Owing to the different DIFs of steel reinforcement of the various models, these curves separated obviously. When the steel reinforcement of the bottom reached their tensile strength, these curves reached their top points. With increased displacement loading, the force decreased and these curves became descending because of the negative stiffness. Compared with the rate-independent model, the numerical curves, considering the rate-dependence of concrete and steel reinforcement, could better simulate the experimental results, especially at the high loading rates. However, with increasing loading rate, the calculated results of the ultimate displacement of the RC beam were less than the experimental results. This is because these calculated models did not consider the effect of loading rate on the ultimate displacement of the steel reinforcement.

Table 7 Effect of loading rates on the dynamic strengths of RC beams

Strength	Loading rate (mm/s)	Experimental results	Numerical results			
			Model I	Model II	Model III	Model IV
Cracking strength (kN)	0.1	24.48	27.30	27.31	27.31	27.31
	0.5	25.65	27.30	27.31	27.31	27.31
	1	26.12	27.30	27.31	27.31	27.31
	5	27.85	27.30	27.31	27.31	27.31
	10	27.93	27.30	27.31	27.31	27.31
Yield strength (kN)	0.1	61.38	58.75	54.85	63.72	65.68
	0.5	64.29	58.75	55.32	64.16	66.32
	1	68.77	58.75	57.09	64.53	66.40
	5	70.82	58.75	59.05	64.88	68.21
	10	71.11	58.75	62.96	65.02	68.65
Ultimate strength (kN)	0.1	87.51	97.84	88.75	97.30	98.88
	0.5	88.34	97.68	89.33	98.13	99.01
	1	94.98	97.45	90.96	99.54	99.86
	5	95.59	97.36	93.22	101.35	102.02
	10	99.20	97.33	98.46	102.82	100.73

5.3 Effect of loading rates on the dynamic strengths of the RC beam

Table 7 listed the comparison of numerical results and experimental results on the cracking strength, the yield strength and the ultimate strength of RC beams at five various loading rates. It was clear that the cracking strength of the numerical results was almost the same, which was different from the experiment results. The reason was that the cracking strength of the RC beam was determined based on the tensile strength of concrete, and the effect of strain rates on the tensile strength of concrete wasn't obvious and the cracking zone was narrow. The yield strength and the ultimate strength in the numerical results increased with increasing loading rates, which was similar to that in the experimental results. However, the strength increasing factor of the numerical results was smaller than that of the experimental result at the same loading rate. Compared with

Table 8 Effect of loading rates on the deformation behaviours of RC beams

Displacement	Loading rate (mm/s)	Experimental results	Numerical results			
			Model I	Model II	Model III	Model IV
Cracking Displacement (mm)	0.1	0.59	0.40	0.41	0.41	0.40
	0.5	0.62	0.40	0.41	0.41	0.40
	1	0.69	0.40	0.41	0.41	0.40
	5	0.74	0.40	0.41	0.41	0.40
	10	0.78	0.40	0.41	0.41	0.40
Yield Displacement (mm)	0.1	3.40	2.97	3.01	3.75	3.95
	0.5	3.52	2.97	3.07	3.90	3.94
	1	3.78	2.97	3.15	3.80	3.78
	5	3.98	2.97	3.14	3.86	3.76
	10	4.05	2.97	3.25	3.85	3.46
Ultimate Displacement (mm)	0.1	19.74	24.17	23.30	24.22	24.00
	0.5	23.29	23.71	22.41	24.03	23.58
	1	25.02	23.19	22.27	23.75	22.75
	5	25.56	23.47	21.94	23.43	22.94
	10	26.80	23.44	22.68	22.78	20.60

Malvar's model and the CEB model, the yield strength of the CEB was bigger than that of Malvar's model but the ultimate strength was smaller, which was consistent with the effect of the loading rate on the steel reinforcement in these models.

5.4 Effect of loading rates on the deformation behaviours of the RC beam

Table 8 lists the comparison of numerical results and experimental results of the mid-span cracking displacement, the mid-span yield displacement and the mid-span ultimate displacement of the RC beams at five various loading rates. It was clear that the cracking displacement of the numerical results was almost the same, due to the same reason as for the cracking strength. The yield and ultimate displacement of RC beams increased slightly with increasing loading rate. The displacement increasing factor was obviously smaller that the strength increasing factor because the steel model did not consider the effect of loading rate on the deformation of steel reinforcement.

6. Conclusions

Based on the experimental and numerical results, the following conclusions were drawn:

• The reduction of natural frequency depends on the crack depth and crack location. (1) The failure configurations of five RC beams were the same at various loading rates. The width of the crack decreased slightly with increasing loading rates and the cracks distributed more uniformly.

• The crack, yield and ultimate strength of the RC beams increased with increasing loading rate, and the strength increasing factor followed linearly with the logarithmic of the loading rate. The crack, yield and ultimate displacement of RC beams increased with increasing loading rate.

• The displacement ductility factor and the energy dissipation capacity of the RC beams increased dramatically with increasing loading rate.

• The numerical results could describe the loading deformation curves and the crack process of the RC beam at various loading rates.

• The numerical results showed that the yield and ultimate strength increased obviously with the increasing loading rates, while the yield and ultimate displacement increased slightly.

Acknowledgments

This study was funded by the National Science Foundation of China under grant No. 51178082 and No. 51421064. The staff of the department of Civil Engineering at the Shenyang Jianzhu University supported the experimental studies; their efforts are gratefully acknowledged. The first author spent a one-year sabbatical in concrete structure research at the University of Houston, supported by the China Scholarship Council.

Notation

F_c	The crack strength of RC beam, kN
F_y	The yield strength of RC beam, kN
F_u	The ultimate strength of RC beam, kN
r_s	The quasi static loading rate, mm/s
r_d	The dynamic loading rate, mm/s
Δ_f	The failure displacement of RC beam, mm
Δ_y	The yield displacement of RC beam, mm
μ_Δ	The displacement ductility factor of RC beam
φ	Yield function of concrete material
J_2	The second invariable of the deviatoric stress tensor
I_1	The first invariable of stress tensor, MPa
f_t	The tensile strength of concrete, MPa
f_c	The compressive strength of concrete, MPa
$\dot{\varepsilon}_s$	Dynamic strain rate of steel reinforcement, s^{-1}
$\dot{\varepsilon}_{s0}$	Quasi-static strain rate of steel reinforcement, s^{-1}
f_{ys}	Static yield strength of steel reinforcement, MPa
f_{yd}	Dynamic yield strength of steel reinforcement, MPa
f_{us}	Static ultimate strength of steel reinforcement, MPa
f_{ud}	Dynamic ultimate strength of stee l reinforcement, MPa
$\dot{\delta}$	Mid-span loading rate of RC beam, m/s
$\dot{\varepsilon}_p$	The peak strain rate of the tensile reinforcement, s^{-1}

References

Abbas, A.A., Pullen, A.D. and Cotsovos, D.M. (2010), "Structural response of RC wide beams under low-rate and impact loading", *Mag. Concrete Res.*, **62**(10), 723-740.

Adhikary, S.D., Li, B. and Fujikake, K. (2012), "Dynamic behavior of reinforced concrete beams under varying rates of concentrated loading", *J. Imp. Eng.*, **47**(4), 24-38.

Adhikary, S.D., Li, B. and Fujikake, K. (2014), "Effects of high loading rate on reinforced concrete beams", *ACI Struct. J.*, **111**(3), 651-660.

Adhikary, S.D., Li, B. and Fujikake, K. (2013), "Strength and behavior in shear of reinforced concrete deep beams under dynamic loading conditions", *Nucl. Eng. Des.*, **259**(6), 14-28.

Al-Haddad, M.S. (1995), "Curvature ductility of reinforced concrete beams under low and high strain rates", *ACI Struct. J.*, **92**(5), 526-534.

Beshara, F.B.A. and Virdi, K.S. (1992), "Prediction of dynamic response of blast-loaded reinforced concrete structures", *Comput. Struct.*, **44**(1), 297-313.

Bischoff, P.H. and Perrry, S.H. (1991), "Compressive behaviour of concrete at high strain rates", *Mater. Struct.*, **24**, 425-450.

Cadoni, E., Labibes, K. and Albertini, C. (2001), "Strain-rate effect on the tensile behaviour of concrete at different relative humidity levels", *Mater. Struct.*, **34**(1), 21-26.

CEB 187 (1988), *Concrete Structures under Impact and Impulsive Loading, Comité Euro-International du Béton*, Lausanne, Switzerland.

Cotsovos, D.M., Stathopoulos, N.D. and Zeris, C.A. (2008), "Behavior of RC beams subjected to high rates of concentrated loading", *J. Structs Eng.*, **134**(12), 1839-1851.

Domenico, A., Ezio, C. and Andrea, P. (2009), "Tensile high strain-rate behavior of reinforcing steel from an existing bridge", *ACI Struct. J.*, **106**(4), 523-529.

Fang, Q., Liu, J.C., Zhang, Y.D. and Qian, Q.H. (2001), "Finite element analysis of failure modes of blast-loaded r/c beams", *Eng. Mech.*, **18**(2), 1-8.

Fang, Q. and Qian, Q.H. (1997), "Discussion on the consideration of the rate sensitivity in design of protective structures", *Expl. Shock Wave.*, **17**(2), 104-110.

Farag, H.M. and Leach, P. (1996), "Material modelling for transient dynamic analysis of reinforced concrete structures", *J. Numer. Meth. Eng.*, **39**(12), 2111-2129.

Fu, H.C., Erki, M.A. and Seckin, M. (1991), "Review of effects of loading rate on reinforced concrete", *J. Struct. Eng.*, **117**(12), 3660-3679.

Fujikake, K., Li, B. and Soeun, S. (2009), "Impact response of reinforced concrete beam and its analytical evaluation", *ASCE J. Struct. Eng.*, **135**(8), 938-950.

Fujikake, K., Senga, T., Ueda N., Ohno, T. and Katagiri, M. (2006b), "Study on impact response of reactive powder concrete beam and its analytical model", *J. Adv. Concrete Technol.*, **4**(1), 99-108.

Fujikake, K., Senga, T., Ueda, N., Ohno, T. and Katagiri, M. (2006a), "Nonlinear analysis for reactive powder concrete beams under rapid flexural loadings", *J. Adv. Concrete Technol.*, **4**(1), 85-97.

Fukuda, T., Sanuki, S., Miyakawa, M. and Fujikake, K. (2011), "Influence of loading rate on shear failure resistance of RC beams", *Appl. Mech. Mater.*, **82**, 229-234.

GB 50010-2010 (2011), *Code for Design of Concrete Structures*, Ministry of Housing and Urban-Rural Development, Beijing, China.

Ghabossi, M.W.A. and Isenberg, J. (1984), "R/C structures under impulsive loading", *J. Struct. Eng.*, **110**(3), 505-522.

Krauthammer, T., Bazeos, N. and Holmquist, T.J. (1986), "Modified SDOF analysis of RC box-type structures", *J. Struct. Eng.*, **112**(4), 726-744.

Krauthammer, T. (1984), "Shallow-buried RC box-type structures", *J. Struct. Eng.*, **110**(3), 637-651.

Kulkarni, S.M. and Shah, S.P. (1998), "Response of reinforced concrete beams at high strain rates", *ACI Struct. J.*, **95**(6), 705-715.

Kunnath, S.K. and Reinhorn, A.M. (1990), "Model for inelastic biaxial bending interaction of reinforced concrete beam-columns", *ACI Struct. J.*, **87**(3), 284-291.

Li, H.N. and Li, M. (2013), "Experimental and numerical study on dynamic properties of RC beam", *Mag. Concrete Res.*, **65**(12), 744-756.

Li, M. and Li, H.N. (2010), "Dynamic test and constitutive model for reinforcing steel", *Chin. Civil Eng. J.*, **43**(4), 70-75.

Malvar, L.J. (1998), "Review of static and dynamic properties of steel reinforcing bars", *ACI Mater. J.*, **95**(5), 609-616.

Nürnbergerová, T., Krizma, M. and Hájek, J. (2001), "Theoretical model of the determination of the deformation rates of RC beams", *Constr. Build. Mater.*, **15**(4), 169-176.

Oh, B.H. (1987), "Behaviour of concrete under dynamic tensile loads", *ACI Mater. J.*, **84**(1), 8-13.

Pandey, A.K. (2011), "An iterative approach for curvature ductility of RC beams at high strain rates", *J. Struct. Eng.*, **38**(4), 307-317.

Pandey, A.K. (2013), "Flexural ductility of RC beam sections at high strain rates", *Comput. Concrete*, **12**(4), 537-552.

Rossi, P. and Toutlemonde, F. (1996), "Effect of loading rate on the tensile behaviour of concrete: Description of the physical mechanisms", *Mater. Struct.*, **29**(2), 116-118.

Rossi, P., Van, M. and Jan, G.M. (1994), "Effect of loading rate on the strength of concrete subjected to uniaxial tension", *Mater. Struct.*, **27**(5), 260-264.

Sziveri, J., Topping, B.H.V. and Ivanyi, P. (1999), "Parallel transient dynamic non-linear analysis of reinforced concrete plates", *Adv. Eng. Softw.*, **30**(9-11), 867-882.

Tedesco, J.W., Ross, C.A., McGill, P.B. and O'Neil, B.P. (1991), "Numerical analysis of high strain-rate concrete direct tension tests", *Comput. Struct.*, **40**(2), 313-327.

Valipour, H.R., Huynh, L. and Foster, S.J. (2009), "Analysis of RC beams subjected to shock loading using a modified fibre element formulation", *Comput. Concrete*, **6**(5), 377-390.

Wang, L.H., Zhou, X.Y., Yan, W.M. and Yu, M. (2006), "Test study on the nonlinear dynamic characteristics of reinforced concrete beams", *J. Seismol. Res.*, **29**(1), 65-71.

Xiao, S.Y., Li, H.N. and Lin, G. (2008), "Dynamic behaviour and constitutive model of concrete at different strain rates", *Mag. Concrete Res.*, **60**(4), 271-278.

Zielinski, A.J., Reinhardt, H.W. and Körmeling, H.A. (1981), "Experiments on concrete under uniaxial impact tensile loading", *Mater. Struct.*, **14**(2), 103-112.

HK